Stress induced birefringence of glass-to-metal bonded components

Stress induced birefringence of glass-to-metal bonded components

Hann, Samuel, MaCleod, Nathan, Morawska, Paulina, Dzipalski, Adrian, Carter, Richard, et al.

Samuel N. Hann, Nathan MaCleod, Paulina O. Morawska, Adrian Dzipalski, Richard M. Carter, Ian Elder, Robert A. Lamb, M.J. Daniel Esser, Duncan P. Hand, "Stress induced birefringence of glass-to-metal bonded components," Proc. SPIE 11540, Emerging Imaging and Sensing Technologies for Security and Defence V; and Advanced Manufacturing Technologies for Micro- and Nanosystems in Security and Defence III, 115400W (20 September 2020); doi: 10.1117/12.2574219

SPIE.

Event: SPIE Security + Defence, 2020, Online Only

Stress Induced Birefringence of Glass-to-Metal Bonded Components

Samuel N. Hann[1], Nathan Macleod[1], Paulina O. Morawska[1], Adrian Dzipalski[1], Richard M. Carter[1], Ian Elder[2], Robert A. Lamb[2], M. J. Daniel Esser[1], Duncan P. Hand[1]
1- Institute of Photonics and Quantum Sciences, Heriot-Watt University, Edinburgh, EH14 4AS, UK
2- Leonardo MW Ltd., 2 Crewe Road North, Edinburgh, EH5 2XS

ABSTRACT

We report on the stress induced birefringence of 10 mm BK7 cubes bonded to 15 mm x 15 mm x 5 mm aluminium coupons using ultrashort pulse laser welding, hydroxide catalysis bonding, and an optical adhesive using a standard approach used in industry. It was observed that ultrashort pulse laser welding results in a low level of stress induced birefringence within an 85% optical aperture of the 10 mm cube. These levels are suitable for use in photography and microscopy applications as defined by the relevant ISO standard for permissible stress induced birefringence limits in optics. Hydroxide catalysis bonding was shown to approach and possibly exceed this limit, however, it must be noted that the bonding area of the hydroxide catalysis samples greatly exceeds that of the welding and adhesive bonded samples by a factor of 20 and thus will likely experience grater mechanical stress from defects on the metal surface.

Keywords: Lasers and laser optics; Optical design and fabrication; Laser materials processing; Birefringence; Stress induced birefringence; Circular polariscope; Polarisation.

1. INTRODUCTION

Ultrashort pulse laser welding and other novel methods of bonding dissimilar materials such as hydroxide catalysis bonding have been presented as attractive alternatives to the currently-used adhesive bonding of glass-to-metal components e.g. in the fabrication of lasers and optical systems. Adhesive bonding can suffer from performance and reliability issues such as outgassing, creep and degradation with age[1]. The bonding process can also be labour intensive when ensuring consistent deposition and curing of the adhesive.

Although interest in ultrashort pulse laser welding and hydroxide catalysis as viable bonding methods have been gaining momentum[2-4], it is important to quantify the impact of any stress induced by the bonding process on the optical performance of the component. We therefore implemented a polariscope for stress-induced birefringence analysis of 10 mm BK7 glass cubes bonded to 15 mm x 15 mm x 5 mm aluminium coupons using the Patterson and Wang 6-step method[5] to calculate the stress induced retardation present in the bonded samples. We have applied this measurement system and analysis technique to laser-bonded samples, hydroxide catalysis bonded samples[4], and to samples adhesively bonded with a standard approach used in industry[6]. The results of this analysis are presented in terms of ISO Standard for stress birefringence in optics[7].

2. ULTRASHORT PULSE LASER WELDING METHOD

Ultrashort pulse laser welding has been reported to be capable of achieving a strong stable bond for optimised laser welding parameters, average power of the beam used for welding, the focal plane of the beam with respect to the metal-glass interface, weld translation speed and the applied clamping pressure during the welding process[2-3]. In brief the welding method requires the glass and metal surfaces to be carefully cleaned in order to be free from scratches, dust and other particulates. The glass and metal are then clamped with <0.8 bar to ensure close contact with a sub-micron gap between the surfaces[8]. A pulsed near-infrared laser with a pulse duration of 6 ps, repetition rate of 400 kHz and 1030 nm wavelength is then used to write a centralised weld spiral at a translation speed of 2 mms^{-1}, with 2.5 mm and 0.4 mm outer and inner diameter respectively, and a pitch of 0.156 mm. The welding process takes approximately 40 seconds with pre-prepared and clamped samples.

Emerging Imaging and Sensing Technologies for Security and Defence V; and Advanced Manufacturing Technologies for Micro-and Nanosystems in Security and Defence III, edited by G. S. Buller et al, Proc. of SPIE Vol. 11540
115400W · © 2020 SPIE · CCC code: 0277-786X/20/$21 · doi: 10.1117/12.2574219

3. HYDROXIDE CATALAYSIS BONDING METHOD

Hydroxide catalysis bonding is another emerging optics bonding technique which has been used to bond stable optical system components for use in space borne systems[4]. The technique involves application of a silicate solution to the rigorously cleaned and prepared surfaces being bonded. These are then brought into contact, aligned, and held in place for dehydration of the silicate solution. The dehydration process can take up to 4 weeks, but significant strength can be achieved after 1 day. In the case of the aluminium coupon, as it cannot form a silicate-like network but as it does have an oxidised surface it chemically binds to the existing silicate-like network of the BK7 cube if the correct silicate solution is used[4]. Depending on the silicate solution used the global surface flatness required for bonding is between $\lambda/4$ and $\lambda/10$ where $\lambda = 600$ nm[4]. Two machined surface types were investigated using 22 samples of each surface, the first surface was milled, the second was milled and then finely cut using a diamond fly cutting process to provide a very flat bonding surface. Due to the nature of this bonding method the bonded area is the full 100 mm^2 surface area of the glass cube compared to the 4.9 mm^2 surface area of the welded samples.

4. ADHESIVE BONDING METHOD

Common practice when using adhesives to bond optics to support structures is to first coat the metal with a passivation substance to protect the metal surface and enhance the bond quality. As the hydroxide catalysis and laser welded samples used untreated metal surfaces the adhesive bonded samples consist of a control group with an untreated metal surface and another group which has been treated with SurTec 650[9] to more accurately represent an industrial component. The bonding method involves cleaning the glass and metal to be free from dust and particulates. A ~0.5 µL drop of Norland 61 optical adhesive[6] is then placed at the centre of the metal surface with a 106 µm filament adequately spaced from the drop and looped around it to act as a spacer for a consistent bond height to obtain an approximately 2.5 mm diameter adhesive spot bond when the glass is placed and aligned on top of the metal coupon. A UV gun is used for 5 mins to partially cure the adhesive while the sample is clamped in place. The part is then placed onto a hot plate to heat cure at 50ºC for 12 hours to chemically bind Norland 61 to the glass.

5. MEASUREMENT OF STRESS INDUCED BIREFRINGENCE

Introduction

It is anticipated that the bonding of glass to metal will cause stress at the bond site which will propagate through the glass resulting in stress induced birefringence being observed, this is particularly of concern with direct bonding methods where no interlayer is used such as hydroxide catalysis and laser welding. Any stress induce birefringence in the clear optical aperture of the optic will have a negative impact on the wave front quality of any propagating light, this will be more significant in polarisation sensitive instruments. Therefore, a method of characterising the stress induced birefringence introduced by the bonding methods was developed using a circular polariscope and the Patterson & Wang 6-step method[5,10].

Circular Polariscope Setup

Typically a circular polariscope consists of a pair of quarter waveplates (QWP) bracketing the sample under analysis, these are then bracketed by a pair of polarisers with a monochromatic light source at one end with accompanying collimation optics and a camera with appropriate objective lens at the other[10]. Our setup deviates slightly from this by inserting a half-wave plate (HWP) between the 2nd quarter wave-plate and the analyser (2nd polariser), see Figure 1. This was done to compensate for errors introduced by rotating the analyser.

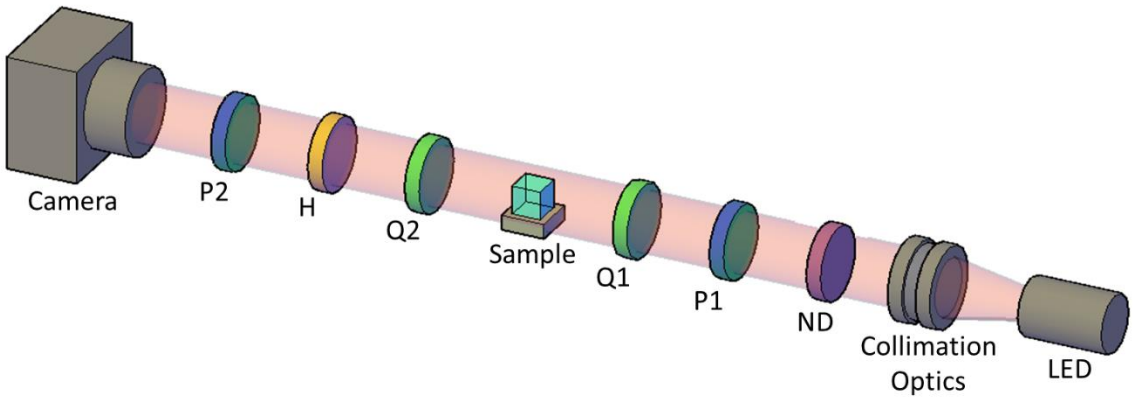

Figure 1: Optical layout of automated circular polariscope setup, consisting of a 635 nm light emitting diode (LED), beam conditioning optics, neutral density (ND) filters, polarisers (P), quarter-wave plates (Q), half-wave plate (H), and the adjustable zoom lens imaging the sample onto the CCD camera.

Patterson & Wang 6-Step Method

The Patterson & Wang 6-step method[5] is strictly speaking a 2D birefringence measurement technique, it can however be applied to 3D samples with the caveat that the resulting retardation map contains no information regarding depth, it is the total measured retardation across the samples depth. We can therefore comment on the relative increase in birefringence from the bulk glass when it is bonded to the metal rather than measuring the birefringence of the bond directly.

Table 1: Table of 6 step analysis optics angles, all angles are anti-clockwise from the horizontal when viewed through the camera.

Step	1st Polarizer	QWP 1	QWP 2	HWP	2nd Polarizer
I_1	90	135	0	22.5	0
I_2	90	135	0	157.5	0
I_3	90	135	0	0	0
I_4	90	135	45	22.5	0
I_5	90	135	90	45	0
I_6	90	135	135	157.5	0

As the optical layout of our polariscope differs somewhat from a typical circular polariscope we have adjusted the associated optic angles for each step of the analysis to compensate, the new angles are shown in Table 1. For each step an image of the sample is taken using the camera, once all 6 images have been taken they are used in Equations 1 and 2 to evaluate the shift in polarisation of the two orthogonal polarisation states, the fast and slow axis. Converting the shift in polarisation from radians to optical path difference (OPD) in nanometres using Equation 3 enables a comparison to the ISO standard for stress induced birefringence[7] where the polariscope source wavelength is 625 nm.

$$\theta = \frac{1}{2} Atan\left(\frac{I_5 - I_3}{I_4 - I_6}\right) \tag{1}$$

$$\delta_C = Atan2\left(\left(\left((I_5 - I_3) \times Sin(2\theta)\right) + \left((I_4 - I_6) \times Cos(2\theta)\right)\right),\ I_1 - I_2\right) \tag{2}$$

where: δ_c is the retardation of each pixel in radians, θ is the angle between the principle measuring angle and the birefringent axes of the sample and I_i the Intensity of each individual pixel in image i, where i = 1:6.

$$R(nm) = \frac{\lambda(nm)R(rad)}{2\pi} \tag{3}$$

where: R(nm) is the is the retardation of each pixel in nanometres, R(rad) is the is the retardation of each pixel in radians and λ(nm) is the peak wavelength of the monochromatic light source used in the polariscope in nanometres.

Retardation Analysis Method

The analysis of the retardation maps begins by finding the glass cube edges in the retardation map and then performing a background subtraction by sampling the retardation level outside the glass cube and then subtracting this from the retardation map, zeroing the background level of the map. The clear aperture of the cube is then defined at its centre of with a diameter that is 85% of its height, see Figure 2. The retardation map contains both a positive and negative shift in retardation as seen in Figure 2. A positive value implies the extraordinary axis has a higher refractive index than the ordinary ray, and a negative retardation implies the extraordinary axis has a lower refractive index than the ordinary ray. In order to determine the overall mean change in optical path difference as a result of the stress induced birefringence in the clear aperture of the sample the root mean square (RMS) of the retardation in the clear aperture is calculated.

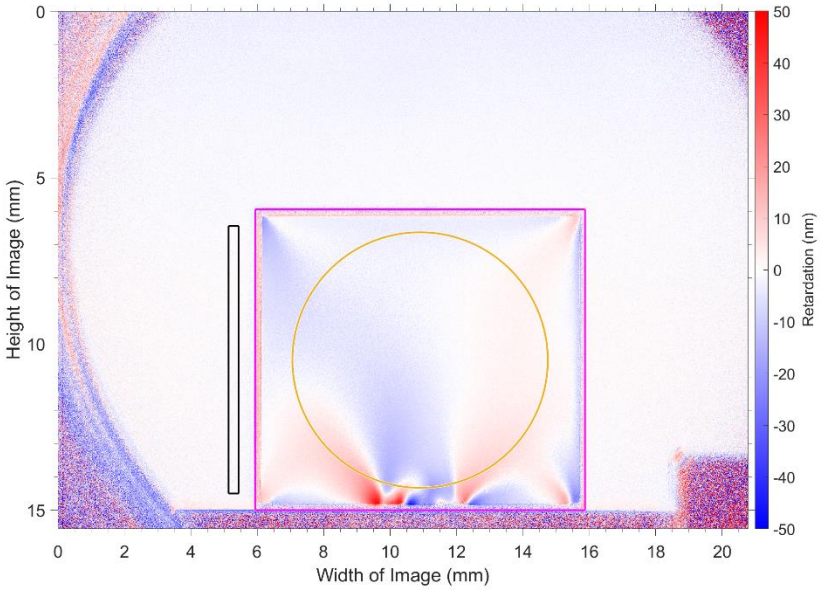

Figure 2: Retardation map (OPD in nm) showing the areas used in the retardation map analysis, background sampling area (**Black**), cube area (Magenta) and clear optical aperture (Yellow).

Cumulative distribution function of a Normal Gaussian Distribution Fitting

While evaluating the distribution of samples from a set with identical bond parameters it was observed that the RMS retardation in the clear optical aperture follows a cumulative distribution function (CDF) of a normal gaussian distribution. It would appear that in this case the central limit theorem[11] holds which states that when independent variables are summed, they tend towards a normalized distribution even when the original variables are not normally distributed. From the fitted curve a maximum retardation for each sample set can be obtained. Therefore fitting the distribution of the RMS retardation in the clear optical aperture of each sample set facilitates a comparison between the different welding parameters used as well as a comparison between the 3 bonding methods being investigated and the RMS retardation in the clear optical aperture of the bulk glass.

6. RESULTS

Ultrashort Pulse Laser Welding

A parameter map consisting of 16 sets of welding parameters combinations with 5 samples per set ranging from -150 µm to -550 µm and 2 W to 5 W in focal plane and average power respectively was created to narrow down the parameter space to determine likely candidates for optimised welding parameters for further investigation. To be statistically meaningful each set should ideally include approximately 20 samples. As this would be prohibitively expensive and time consuming for each of the 16 parameter sets a smaller sample set of 5 was used and will be followed up with larger sample sets in a future study.

Fitting the 16 sets of samples for given parameter combinations it was determined that the 3 with the lowest retardation are 5 W -550 µm, 5 W -150 µm, and 4 W -150 µm. Shear testing the samples showed that 5 W -550 µm was an unstable bond as most of the samples failed while being mounted in the shear testing rig with the exception of one which was exceptionally strong. Shear testing the other two sets showed that by contrast they were strong and had a similar shear strength to each other suggesting that the focal plane is more critical to welding success than the average power used. Investigating a fixed focal plane of -150 µm and varying average power, see Figure 3, we see that the 4 W and 5 W sets are indeed very similar in terms of the RMS retardation in the clear optical aperture and thus make good candidates for further study with a maximum change in optical path of 6.0 nm and 7.1 nm respectively.

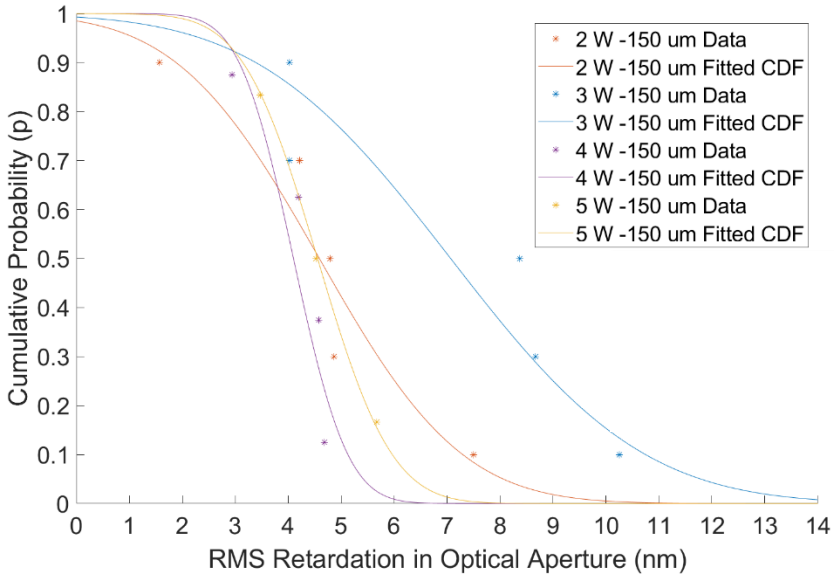

Figure 3: Distribution plot of the RMS retardation in the optical aperture for a fixed focal plane of -150 µm and average power ranging from 2 W to 5 W.

Hydroxide Catalysis Bonding

The milled and milled plus diamond fly cut samples were studied and plotted as discussed with the resulting CDF fit plot shown in Figure 4. The diamond fly cut surface performed better than the milled surface with a more consistent, lower distribution of RMS retardation. This was to be expected as the hydroxide catalysis bonding process requires a very flat bonding surface, although the rougher milled surface did bond its increased roughness induced more stress birefringence at the bond site resulting in a higher retardation of 12.4 nm compared to 9.9 nm with the diamond fly cut.

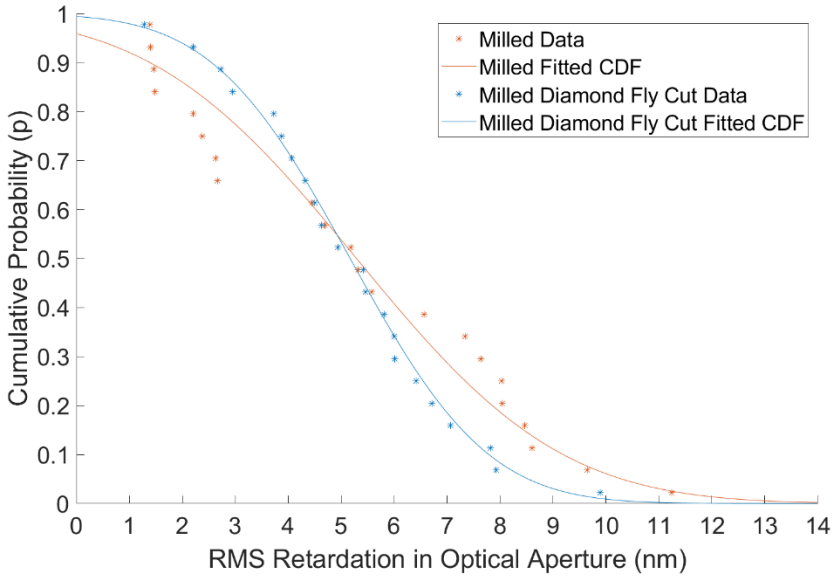

Figure 4: Distribution plot of the RMS retardation in the optical aperture for the hydroxide catalysis bonded samples.

Adhesive Bonded

Figure 5 shows the CDF fit for the RMS retardation in the optical aperture, in terms of the stress birefringence the treated and un-treated surface yield near identical curves with a maximum retardation of 3.5 nm and 3.7 nm respectively. As the adhesive acts as an interlayer the stress on the bulk glass from the bond is minimal resulting in a consistent low distribution of RMS retardation in the optical aperture independent of surface finish.

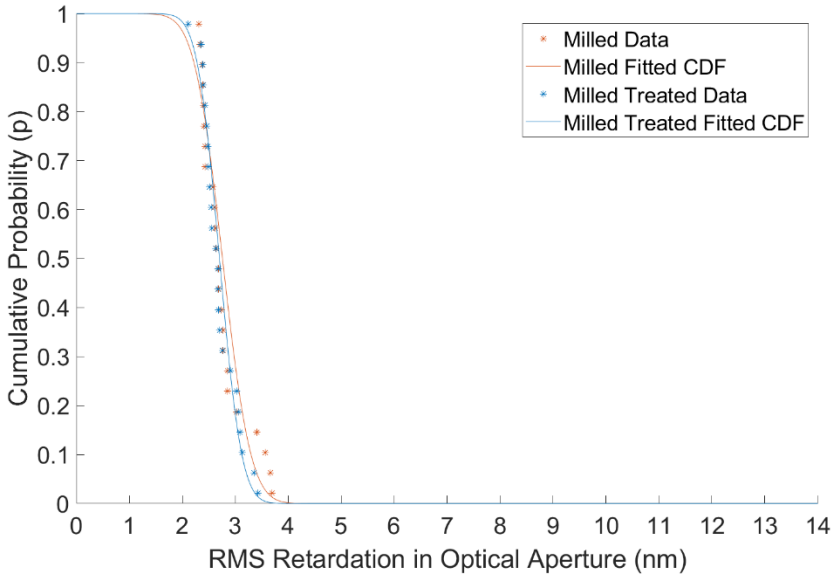

Figure 5: Distribution plot of the RMS retardation in the optical aperture for the adhesive bonded samples.

Comparison of Bonding Method Results

Owing to a change in supplier multiple brands of BK7 cubes were used, comparing the CDF curves of RMS retardation for these and the treated adhesively bonded, optimised welding parameters and diamond fly cut hydroxide catalysis samples the effect of the bond type on the stress induced birefringence in the optical aperture can be ascertained, see Figure

6. The adhesive bond appears to have a minimal effect of the clear optical aperture with its distribution of RMS retardation closely matching that of the bulk glass distributions, with a maximum retardation of 3.1 nm and 3.3 nm for the two glass brands and 3.5 nm for the milled and treated adhesive spot bonded samples. The welds in contrast appear to have a significant effect on the clear optical aperture compared to the adhesive bonds with a maximum retardation of 6 nm and 7.1 nm for 4 W and 5 W welds respectively. However, this effect is lower than the hydroxide catalysis bonds which showed the highest RMS retardation distribution with a maximum retardation of 9.9 nm for the milled and diamond fly cut surface.

In relation to the ISO standard[7] for stress induced birefringence the maximum permissible retardation for precision optics and astronomical optics is 5 nm·cm^{-1}, for photography and microscopy type applications this limit is increased to 10 nm·cm^{-1}. Therefore, adhesive bonding and ultrashort pulse laser welding can be used to mount 10 mm thick optics using a 2.5 mm diameter bond as described for use in the latter application types with adhesive bonding also being suitable for the former application types. Hydroxide catalysis was shown to produce samples with a maximum retardation which approaches the latter limit of 10 nm·cm^{-1}, however, it is of import to note that unlike the adhesive bonded or ultrashort pulse laser welded samples the hydroxide catalysis samples were bonded using the full 100 mm^2 surface area of the BK7 cube as opposed to a 4.9 mm^2 spot bond. This may have a significant impact on the stress induced birefringence as the larger surface area may result in a higher mechanical stress applied from peaks on the metal surface to the glass.

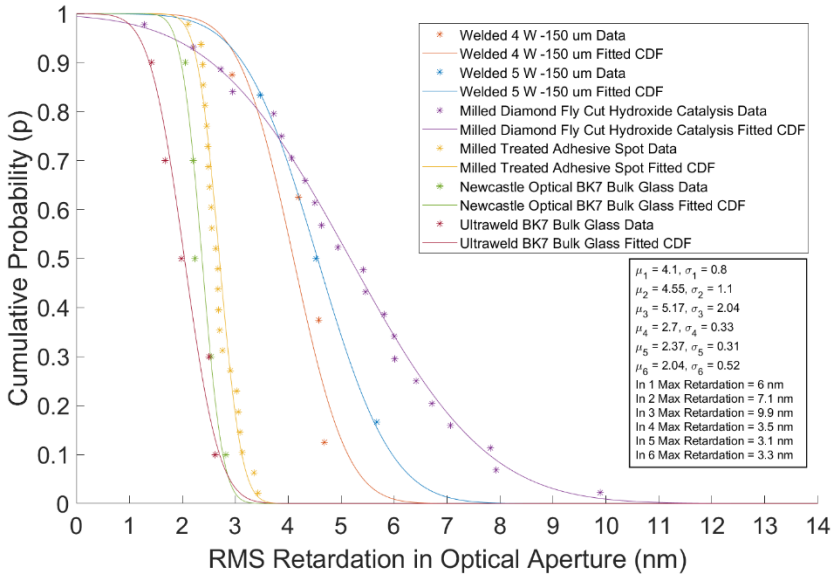

Figure 6: comparative plots of the distribution of the optimised welded sample sets, the treated adhesive bonded samples sets, the diamond fly cut hydroxide catalysis bonded samples sets and the CDF curves for the bulk glass of the two brands of glass cubes used.

7. CONCLUSIONS

A relative comparison between adhesive bonded, ultrashort pulse laser welded, hydroxide catalysis bonded and bulk glass in terms of stress induced birefringence it was observed that adhesive bonding achieves the same order of magnitude of stress birefringence in the optical aperture as the residual stress from production in the bulk glass. Optimized laser welding parameters for ultrashort pulse laser welding achieves a stress induced birefringence in the optical aperture that is approximately double that of the bulk glass and is more dependent on focal plane than the average power of the beam. Hydroxide catalysis exhibits the highest stress induced birefringence of the 3 bond types investigated, this may be due to the 20-fold increase in bond surface area compared to the other two methods which use 2.5 mm spot bonds, high flatness becomes increasingly more important the larger the surface area being bonded, particularly so for the hydroxide catalysis bonding process. In terms of the permissible stress induced birefringence limits in optics as specified in the relevant ISO standard, ultrashort pulse laser welding can be used to mount 10 mm thick optics using a 2.5 mm diameter spiral weld for use in photography and microscopy type applications. Hydroxide catalysis was shown to also be suitable for these type of applications when bonding this material combination, however post bonding quality control will be required to reject a

small percentage of parts that may fail to meet the required retardation level. Reducing the bond surface area may resolve this issue by reducing the stress induced birefringence in the optical aperture to a more acceptable level comparable to the adhesive bonded and welded samples. Further work is required to continue optimising the ultrashort pulse laser welding parameters of 4 W or 5 W at a focal plane of -150 µm, in particular the investigation of larger sample sets to produce a more statistically meaningful understanding of the maximum retardation in the optical aperture as a result of these welds.

ACKNOWLEDGEMENTS

The work presented in this paper was supported by funding from Innovate UK, project 103763, UltraWELD; from EPSRC (EP/R511948/1); and from NMIS (NMIS-IDP/011). The authors would also like to thank Peter MacKay of G&H for his assistance with his technical expertise.

REFERENCES

[1] K. S. Krithika, T. L. Schmitz, P. G. Ifju, and J. G. Daly, "A survey of technical literature on adhesive applications for optics," Proc. SPIE 6665, 666507–666511 (2007).
[2] R. M. Carter, M. Troughton, J. Chen, I. Elder, R. R. Thomson, M. J. D. Esser, R. A. Lamb, & D. P. Hand, "Towards industrial ultrafast laser microwelding: SiO2 and BK7 to aluminum alloy", Applied Optics, vol. 56, pp. 4873-4881. (2017).
[3] R. M. Carter, "UltraWELD: A new method for welding glass and metal", Made For Space, Coventry, United Kingdom, (2019).
[4] E. J. Elliffe, J. Bogenstahl, A. Deshpande, J. Hough, C. Killow, S. Reid, D. Robertson, S. Rowan, H. Ward and G. Cagnoli, "Hydroxide-catalysis bonding for stable optical systems for space", Class. Quantum Gravity 22, S257, (2005).
[5] E. A. Patterson and Z. F. Wang, "Towards full field automated photoelastic analysis of complex components", Strain, 27, 49–53, (1991).
[6] Norland Products, "Norland Optical Adhesive 61", https://www.norlandprod.com/adhesives/NOA%2061.html (25 August 2020).
[7] International Organization for Standardization, "ISO 10110-18:2018 Optics and photonics - Preparation of drawings for optical elements and systems - Part 18: Stress birefringence, bubbles and inclusions, homogeneity, and striae", https://www.iso.org/standard/68155.html#:~:text=Abstract%20Preview,for%20optical%20elements%20and%20systems. (25 August 2020).
[8] Chen, J., Carter, R. M., Thomson, R. R. & Hand, D. P. Avoiding the requirement for pre-existing optical contact during picosecond laser glass-to- glass welding. Opt. Express 23, 18645 (2015).
[9] SurTec, "SurTec 650 - Chromium(VI)-Free Passivation for Aluminium for the Electronics, Automotive and Aerospace Industry", https://www.surtec.com/en/products/product-highlights/628/ (11th July 2020).
[10] K. Ramesh, Digital Photoelasticity: Advanced Techniques and Applications, (Springer-Verlag, 2010).
[11] Montgomery, D. C. & Runger, G. C. Applied statistics and probability for engineers. Wiley (2014).